First-pass and systemic metabolism of cytochrome P450 3A substrates in neonates, infants, and children

Brussee, J.M.

Section II

Systemic CYP3A-mediated metabolism in critically ill children

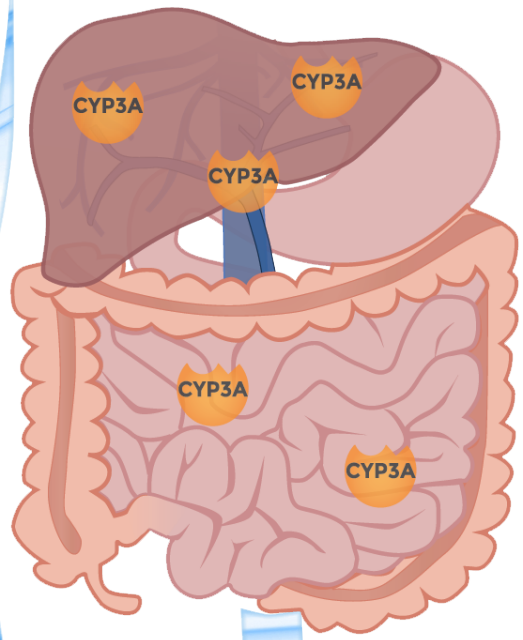

Chapter 3

Inflammation and organ failure severely affect midazolam clearance in critically ill children

Nienke J Vet[1,2*], Janneke M Brussee[3*], Matthijs de Hoog[1,2], Miriam G Mooij[1,4], Carin WM Verlaat[5], Isabel S Jerchel[6], Ron HN van Schaik[7], Birgit CP Koch[8], Dick Tibboel[1,4], Catherijne AJ Knibbe[3,9], Saskia N de Wildt[1,4], On behalf of SKIC (Dutch collaborative PICU research network).

* These authors contributed equally to this work.

[1]Intensive Care, Erasmus MC - Sophia Children's Hospital, Rotterdam, The Netherlands; [2]Department of Pediatrics, Erasmus MC - Sophia Children's Hospital, Rotterdam, The Netherlands; [3]Division of Pharmacology, Leiden Academic Center for Drug Research, Leiden University, Leiden, The Netherlands; [4]Department of Pediatric Surgery, Erasmus MC - Sophia Children's Hospital, Rotterdam, The Netherlands; [5]Intensive Care, Radboud University Nijmegen Medical Center, Nijmegen, The Netherlands; [6]Department of Pediatric Oncology/Hematology, Erasmus MC - Sophia Children's Hospital, Rotterdam, The Netherlands; [7]Department of Clinical Chemistry, Erasmus MC, Rotterdam, The Netherlands; [8]Department of Hospital Pharmacy, Erasmus MC, Rotterdam, The Netherlands; [9]Department of Clinical Pharmacy, St Antonius Hospital, Nieuwegein, The Netherlands

Am J Respir Crit Care Med. 2016 Jul 1;194(1):58-66

ABSTRACT

Rationale: Various in vitro, animal and limited human adult studies suggest a profound inhibitory effect of inflammation and disease on Cytochrome P450 3A (CYP3A)-mediated drug metabolism. Studies showing this relationship in critically ill patients are lacking, while clearance of many CYP3A drug substrates may be decreased, potentially leading to toxicity.

Objectives: To prospectively study the relationship between inflammation, organ failure and midazolam clearance, as validated marker of CYP3A mediated drug metabolism, in critically ill children.

Methods: From 83 critically ill children (median age 5.1 months (range 0.02-202 months)), midazolam plasma levels (n=532), cytokines (e.g. IL-6, TNF-α), C-reactive protein (CRP) and organ dysfunction scores (PRISM II, PIM2, PELOD), as well as number of failing organs were prospectively collected. A population pharmacokinetic model to study the impact of inflammation and organ failure on midazolam pharmacokinetics was developed using NONMEM 7.3.

Main results: In a two-compartmental pharmacokinetic model, body weight was the most significant covariate for clearance and volume of distribution. Both CRP and organ failure were significantly associated with clearance ($p<0.01$), explaining both inter-individual and inter-occasional variability. In simulations a CRP of 300 mg/L was associated with a 65% lower clearance compared to 10 mg/L and three failing organs were associated with a 35% lower clearance compared to 1 failing organ.

Conclusions: Inflammation and organ failure strongly reduce midazolam clearance, a surrogate marker of CYP3A-mediated drug metabolism, in critically ill children. Hence, critically ill patients receiving CYP3A substrate drugs may be at risk of increased drug levels and associated toxicity.

Keywords

Pediatrics; Critical illness; Midazolam; Pharmacokinetics; Inflammation; Cytochrome P450

At a Glance Commentary

Scientific Knowledge on the Subject: Various *in vitro*, animal and limited human adult studies suggest a profound inhibitory effect of inflammation and disease on Cytochrome P450 3A (CYP3A)-mediated drug metabolism. Studies showing this relationship in critically ill patients are lacking.

What This Study Adds to the Field: Inflammation and organ failure strongly reduce midazolam clearance, a surrogate marker of CYP3A-mediated drug metabolism, in critically ill children. Hence, critically ill patients receiving CYP3A substrate drugs may be at risk of increased drug levels and associated toxicity.

INTRODUCTION

Critically ill patients often require life-saving polypharmacy including cardiotonics, antimicrobials and analgo-sedatives. Dependent on the underlying disease state, these patients show large variation in drug disposition and response (1). Understanding the underlying mechanisms contributing to this variation is of importance to ensure the safe and effective use of drugs in this vulnerable population.

Various in vitro, animal and limited human adult studies suggest a profound inhibitory effect of inflammation on drug metabolism by cytochrome P450 (CYP) enzymes. Drug-metabolizing enzymes are downregulated by cytokines released during inflammation (2). Inflammation-related changes in drug disposition have been described for disease states such as auto-immune disease and cancer (3). In addition, hepatic drug metabolism may be affected through a heavy loss of hepatocytes in liver failure or through a still unknown mechanism in renal failure (1, 4).

In children with sepsis and organ failure a two- and fourfold lower antipyrine clearance, respectively, was found compared to non-septic ICU children. In addition, IL-6 was negatively correlated with antipyrine clearance, suggesting inflammation as regulatory mechanism (5). Antipyrine is a global marker of CYP450 metabolism, and individual CYPs appear differentially regulated by inflammation (6). Individual enzymes need to be studied to better understand the substantial impact of drug metabolism on individual CYPs and to individualize drug therapy for individual drugs.

The most abundant CYP, CYP3A4/5, is involved in the metabolism of >50% of therapeutic drugs, of which many are prescribed daily to critically ill patients. Studies showing the relationship between inflammation and CYP3A mediated drug metabolism in critically ill patients are lacking, while clearance of many CYP3A drug substrates may be decreased, potentially leading to toxicity. The benzodiazepine midazolam is metabolized by CYP3A4/5 to a major hydroxylated active metabolite (1-OH midazolam), and subsequently metabolized to 1-OH-midazolam-glucuronide by UGTs and renally excreted (7). The clearance of midazolam to 1-OH-midazolam has been validated as surrogate measure of *in vivo* CYP3A4/5 activity (8). We therefore hypothesized that inflammation is inversely related to midazolam clearance in critically ill pediatric patients. A previous pilot study from our group, in 21 children supports this hypothesis (9). The aim of this study was to prospectively study the relationship between inflammation, organ failure, and midazolam clearance in critically ill children, as a model for CYP3A-mediated drug metabolism. Some of the results of this study have been previously reported in the form of an abstract (10).

METHODS

Subjects and setting

Patients were recruited in the context of a multicenter randomized controlled trial comparing daily sedation interruption plus protocolized sedation to protocolized sedation alone in critically ill children (11). For this pharmacokinetic study, patients from only two of the three participating PICUs in the Netherlands were enrolled: Erasmus MC-Sophia Children's Hospital and Radboud University Nijmegen Medical Center. Approval from each institutional review board and written informed consent from parents or legal representatives was obtained. Details on this study can be found elsewhere (11). A separate power analysis for this pharmacokinetic study was not performed. The sample size was calculated from the study's primary outcome, the number of ventilator-free days (11).

Patients were eligible for the study if they were between 0 and 18 years of age, born at least at 37 weeks of postconceptual age, required mechanical ventilation with an expected duration of at least 48 hours and received sedative drugs. The following exclusion criteria were applied: anticipated death or withdrawal of life support within 48 hours; impossibility of assessing level of sedation due to an underlying neurologic condition; neurological, respiratory or cardiac instability that may not tolerate inadequate sedation; therapeutic hypothermia after cardiopulmonary resuscitation; difficult airway; fixed duration of mechanical ventilation, admission for ECMO; already having been ventilated/sedated for >2 days in a transferring PICU. Midazolam was administered as an intravenous bolus (100 µg/kg) followed by intravenous infusion at a rate of 100 µg/kg/h. Sedation was titrated based on COMFORT-B scores. In the sedation interruption group sedative infusions were interrupted daily.

Measurements

Blood for midazolam concentrations was sampled using an optimized sampling strategy for PK analysis, with 4 samples per day during the first 72 hours and 1 sample per day thereafter at different time points, for up to one week. Inflammatory markers (C-reactive protein (CRP), cytokines (IL-1a, IL-1b, IL-2, IL-4, IL-6, IL-10, TNF-α, IFN-γ, MCP-1, MIP1a, MIP1b, RANTES, IL-8, FGF-b, G-CSF, GM-CSF)), liver and kidney function were determined once daily, CYP3A4*1G, *22 and CYP3A5*3 single nucleotide polymorphisms were also determined. Detailed description of the analytical methods can be found in the supplemental Methods.

Disease severity was scored using validated organ dysfunction scores: the Pediatric Risk of Mortality II (PRISM II) (range 0-100%)(12) and the Paediatric Index of Mortality (PIM2) (range 0-100%)(13) at admission and the Paediatric Logistic Organ Dysfunction (PELOD) score daily (range 0-71)(14). Since the PELOD score is a non-uniform ordered discrete scale, this score was also used to calculate the number of organs failing. If a patient scored the maximum score on an organ subscale (i.e. cardiovascular, renal, respiratory, hematological or hepatic), this was scored as organ failure 'yes'. The total number of organ failures was counted for each measurement (ranging from 0-5).

Pharmacokinetic analysis

Midazolam concentration-time data were analyzed using non-linear mixed effects modelling version 7.3 (ICON, Globomax LLC, Ellicott, MD, USA), complying the latest FDA and EMA guidelines. Model development was in four steps: *1)* selection of a structural model, *2)* selection of an error model, *3)* covariate analysis and *4)* internal validation of the model. For model selection, we used the objective function value (a log-likelihood ratio test, assuming a Chi-squared distribution) to compare nested models. For the structural and error models, a decrease in objective function value (OFV) of 3.84 points was considered statistically significant ($p<0.05$). The optimal model was selected using standard methodology for population PK analysis with NONMEM. The details of model selection and validation can be found in the supplemental Methods.

Once the base model was selected, covariates were tested for their influence on pharmacokinetic parameters. The continuous covariates evaluated were age, weight, CRP, cytokines, PRISM II, PIM2, PELOD, number of organ failures, creatinine, ALAT and albumin. Since the concentration of IL-6 covered a large range, it was log-transformed and as such considered as covariate in the model. Categorical covariates included sex, diagnosis group, co-administration of CYP3A inhibitors (i.e. clarithromycin, voriconazole, fluconazole, erythromycin, haloperidole, metronidazole), study center and CYP3A genetic polymorphisms. Potential covariates were evaluated using forward inclusion and backward elimination with a level of significance of <0.005 (OFV -7.9 points) and <0.001 (OFV -10.8 points), respectively. In addition, inclusion of a covariate in the model had to result in a decline in unexplained inter-individual variability or unexplained inter-occasion variability before it was included in the final model (15, 16). Additional covariates had to reduce the objective function and unexplained variability further to be retained in the model. Next, the model was internally validated as described in the supplement.

Dose simulations

To explore the quantitative impact of relevant covariates on midazolam clearance, identified from the population PK analysis, simulations were performed as follows. Using the currently recommended starting dose in children (a loading dose of 100 µg/kg and a maintenance dose of 100 µg/kg/h for 48 hours) concentration–time profiles were visualized for representative critically ill children with varying body weight, CRP concentrations and organ failure.

RESULTS

Patients and Data

Midazolam concentrations obtained from 83 children admitted to the intensive care unit were included between October 2009 and August 2014. A total of 523 plasma samples were available with a median of 6 (range 1-15) samples per patient. Patients were between 1 day and 17 years old (median age 5.1 months) and body weight ranged from 2.5 to 63 kg (median 5.6 kg). See further Table I.

Table I. Patient characteristics

Characteristics	Total
Number of patients (n)	83
Number of samples (n)	523
Samples/patient*	6 (1 – 15)
Sex (male/female,%)	48/35 (58/42%)
Age (months)*	5.1 (0.02 – 202)
Weight (kg)*	5.6 (2.5 – 63)
Reason admission ICU	
- Respiratory disorder#	58 (70.0%)
- Cardiac disorder##	5 (6.0%)
- Sepsis	8 (9.6%)
- Cardiac surgery	9 (10.8%)
- Non-cardiac surgery	3 (3.6%)
CRP (mg/L)*	32 (0.3 – 385)
IL 6 (ng/L)*	25 (0.55 – 43140)
PRISM II*	17 (0 – 44)
Predicted mortality PIM 2 (%)*	5.3 (0.25 – 33.2)
PELOD*	11 (0 – 41)
Number of failing organs*	2 (0 – 5)

* Data are in median (range). PRISM II=Pediatric Risk of Mortality, PIM 2=Pediatric Index of Mortality, PELOD=Pediatric Logistic Organ Dysfunction, # viral/bacterial pneumonia, ARDS and asthma, ## congenital heart disease and cardiomyopathy.

Model Development and Covariate Analysis

A two-compartmental model described the pharmacokinetics of midazolam well. Inter-individual variability (IIV) for clearance and volume of distribution of the central compartment could be estimated and adding these variability parameters improved the model. Then, the inclusion of inter-occasion variability (IOV) for clearance improved the model. A combined error model, combining a proportional and additive error, was superior over a proportional or additive error model. The inclusion of all these variances in the model resulted in lower residual unexplained errors and improved the model significantly (ΔOFV -119.6, $p<0.01$).

Body weight

The covariate analysis showed that body weight was the most significant covariate resulting in a 76.5 reduction in objective function($p<0.005$). Using body weight as covariate, 32.9% and 43.9% of the IIV in clearance and volume, respectively, of the central compartment was explained (Table II). Therefore, body weight was incorporated in the model (Figure 1a,b and Figure 2a) and with this pediatric base model other covariates were tested to explain more interindividual and interoccasion variability.

Table II. Results of covariate analysis for the two-compartment pharmacokinetic model of miazolam

Covariate	Model	Relationship of covariate	No. of structural parameters	ΔOFV
-	Simple model (without IOV)	-	8	+193.7
Body weight	Pediatric base model (without IOV)	$CL_i=CL_{5kg}\cdot(WT/5)^{k1}$ $V1_i=V1_{5kg}\cdot(WT/5)^{k3}$	10	+117.2
Body weight	Pediatric base model	$CL_i=CL_{5kg}\cdot(WT/5)^{k1}$ $V1_i=V1_{5kg}\cdot(WT/5)^{k3}$	11	-
Organ failure	Pediatric model with organ failure	$CL_i=CL_{5kg}\cdot(WT/5)^{k1}$ with varying CL_{5kg} for varying number of organs failing	14	-34.7
IL6	Pediatric model with inflammatory marker*	$CL_i=CL_{5kg}\cdot(WT/5)^{k1}\cdot(1+l1\cdot(IL6/3.2))$	12	-38.1
CRP	Pediatric model with inflammation	$CL_i = CL_{5kg}\cdot(WT/5)^{k1}\cdot(CRP/32)^{k2}$	12	-59.5
CRP and organ failure	Pediatric model with inflammation and organ failure	$CL_i = CL_{5kg}\cdot(WT/5)^{k1}\cdot(CRP/32)^{k2}$ with varying CL_{5kg} for varying number of organs failing	15	-75.3

*IL6: Interleukin-6 concentrations were log transformed.
ΔOFV: Difference in objective function value compared to Pediatric base model

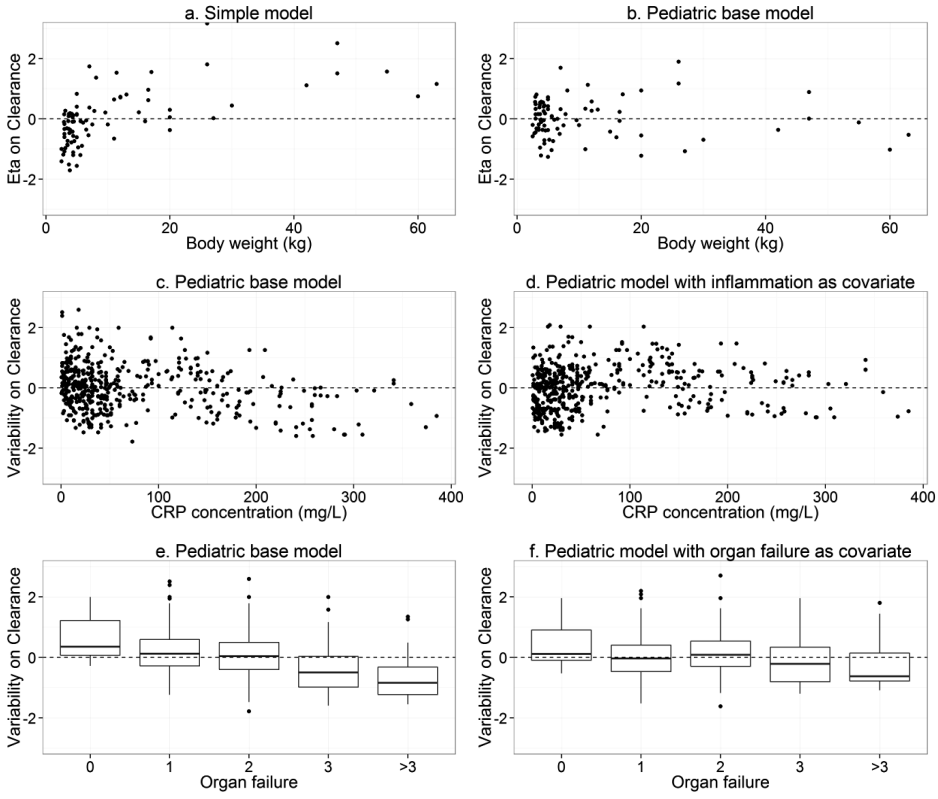

Figure 1. Variability in clearance versus the included covariates before (a,c,e) and after (b,d,f) inclusion of the different covariates. (a, b) Inter-individual variability on clearance versus body weight, before and after inclusion of body weight as covariate on clearance. (c, d) Variability on clearance before and after inclusion of CRP concentration as covariate on clearance. (e, f) Variability on clearance before and after inclusion of organ failure as covariate on clearance. Variability (c, d, e, f) includes inter-individual variability and inter-occasion variability.

Inflammation

The inclusion of the inflammation markers IL-6 and CRP as covariate on clearance resulted in a decrease in the objective function by 38.1 and 59.5 points, respectively (Table II). Since IL-6 and CRP concentrations were highly correlated (Pearson, r=0.6, p<0.001), only CRP concentrations were included as covariate on clearance. Next to a decrease in OFV, incorporating CRP in the model resulted in better goodness-of-fit plots and a decrease in the IOV in clearance of 20.4% (Table II, Figure 1c,d). For higher concentrations of CRP, midazolam clearance was lower (Figure 2b). Figure 3a shows that a CRP of 300 mg/L is associated with a 65.4% lower clearance than a CRP of 10 mg/L. Incorporation of other cytokines (e.g. IL1a, IL1b, IL2, IL4, IL8, IL10 and TNF-α) did neither improve the model significantly, nor explained variability in clearance any further.

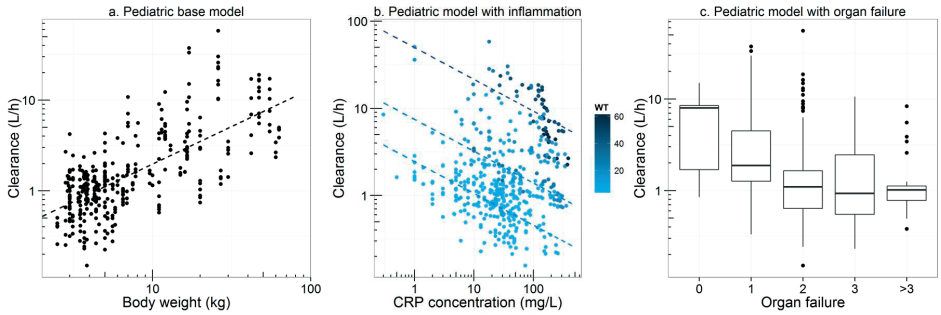

Figure 2. Post-hoc plots for clearance versus the included covariates body weight (a), inflammation marker CRP (b) and organ failure (c). a. Clearance versus body weight. • Individual estimated clearance value for each individual, – Population predicted clearance, predicted with the pediatric base model (table III). b. Clearance versus CRP concentration. • Individual estimated clearance value for each individual at each different CRP measurement in the study. Shaded blue colors indicate body weight (kg) with darker blue for increasing body weight. – Population predicted clearance for an individual of 3.5 (light blue), 10 (intermediate blue) and 60 kg (dark blue), predicted with the model with inflammation (Table III). c. Boxplot of the individual predicted clearance values for each individual on each day in the study versus number of organs failing. Of the 523 plasma samples, 10, 200, 209, 70 and 34 samples were taken from patients with 0, 1, 2, 3 and >3 organs failing respectively.

Organ failure

There was no relation between clearance or volume of distribution and PRISM II or PIM2 scores. The PELOD score correlated negatively with clearance. Including the number of organ failures as covariate in the pediatric model (Figure 1e,f) significantly improved the model (OFV Δ-34.7 points, Table II) and resulted in better goodness-of-fit plots. It lowered the IIV and IOV with 8.6% and 7.8% respectively. The clearance of midazolam decreased with an increasing number of organ failures (Figure 2c). Three failing organs was associated with a 34.7% lower clearance compared to one failing organ (Figure 3b).

Other covariates

Significant differences between study centers were not found. Fourteen patients received a CYP3A inhibitor; this had no effect on midazolam clearance. CYP3A polymorphisms, albumin, creatinine and ALAT concentrations were tested as covariates as well, but did neither improve the model nor explained variability in clearance or volume of distribution.

Table III. Parameter estimates of best models

Parameter	Pediatric base model	Pediatric model with inflammation and organ failure included as covariates	
	Model fit (CV%)	Model fit (CV%)	Bootstrap median (5th-95th percentile)
Clearance	$CL_i = CL_{5kg} \cdot (WT/5)^{k1}$	$CL_i = CL_{5kg} \cdot (WT/5)^{k1} \cdot (CRP/32)^{k2}$ with varying CL_{5kg} for different number of organs failing	
CL_{5kg} (L/h)	1.11 (8%)	ORGF1: 1.29 (14%) ORGF2: 0.96 (13%) ORGF3: 0.84 (27%) ORGF>3: 0.68 (25%)	ORGF1: 1.29 (1.05-1.70) ORGF2: 0.96 (0.78-1.25) ORGF3: 0.83 (0.54-1.30) ORGF>3: 0.67 (0.43-0.99)
k1	0.828 (13%)	1.02 (13%)	1.03 (0.79-1.26)
k2	–	-0.312 (21%)	-0.324 (-0.42- -0.21)
Inter-compartmental clearance			
Q (L/h)	1.57 (43%)	1.52 (34%)	1.37 (0.09-3.43)
Volume of distribution	$V1_i = V1_{5kg} \cdot (WT/5)^{k3}$	$V1_i = V1_{5kg} \cdot (WT/5)^{k3}$	
$V1_{5kg}$ (L)	3.58 (43%)	3.28 (33%)	3.45 (1.79-8.20)
k3	1.32 (19%)	1.34 (17%)	1.30 (0.93-1.74)
V2 (L)	5.35 (21%)	5.44 (16%)	5.13 (0.94-6.71)
Inter-individual variability			
ω^2 CL	0.381 (25%)	0.345 (21%)	0.350 (0.226-0.513)
ω^2 V1	1.14 (59%)	1.19 (50%)	1.07 (0.14-2.06)
Inter-occasion variability			
π^2 CL	0.344 (24%)	0.197 (24%)	0.175 (0.103-0.265)
Residual error			
Proportional	0.096 (15%)	0.098 (15%)	0.095 (0.074-0.121)
Additive (µg/L)	0.121 (18%)	0.138 (19%)	0.139 (0.015-0.210)

CL clearance (L/h), with CL_i the individual predicted clearance of individual *i*, CL_{5kg} the population predicted clearance for a median subject of 5kg, k1 exponent to relate body weight to clearance, k2 exponent to relate CRP concentrations to clearance, Q inter-compartmental clearance (L/h), V1 volume of distribution in the central compartment (L), with $V1_i$ the individual predicted volume of individual *i*, $V_{5\,kg}$ the population predicted volume for a median subject of 5 kg, k3 exponent to relate body weight to volume of distribution, V2 volume of distribution in the peripheral compartment, ω^2 the variance for the inter-individual variability of the parameter mentioned, π^2 the variance for the inter-occasion variability of the parameter mentioned, WT body weight (kg), CRP C-reactive protein concentrations (mg/L), ORGF number of organs with organ failure, with failure defined by a maximum value on the PELOD score for that organ. A bootstrap was performed with 500 times of resampling the dataset.

Final model

Incorporation of both inflammation and organ failure in the model resulted in a lower OFV (Table II) and better description of the data compared to models including

inflammation or organ failure only (goodness-of-fit plots, Suppl. Fig E1). Figure 3c shows that clearance is up to 77.4% lower when patients have both increased CRP and an increased number of organs failing.

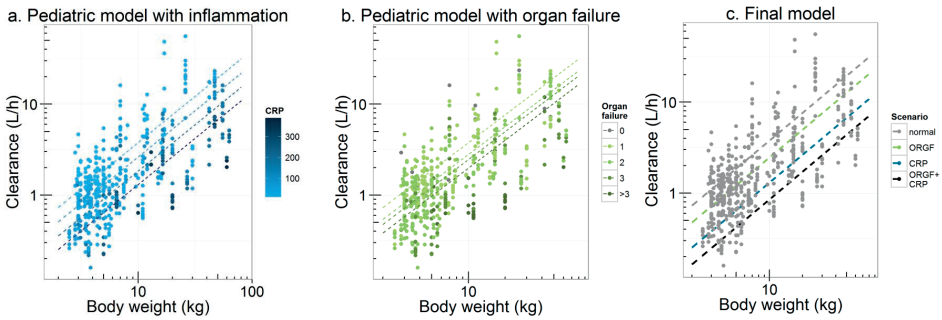

Figure 3. Post-hoc values for clearance versus body weight. Each point represents the posthoc clearance for an individual at a different time point in the study. a. Different colors reflect varying CRP concentrations while the four lines represent the model predictions for CRP concentrations of 10, 32, 100 and 300 mg/L respectively with darker blue lines for increasing CRP concentrations. b. Different colors reflect increasing organ failure while the four lines represent the model predictions for number of organs failing of 1, 2, 3 and >3 respectively with darker green lines for increasing number of organs failing. c. Different colors of the lines reflect different scenarios as predicted by the model. The grey line represents the scenario when the patient has a CRP concentration of 10 mg/L and 1 organ failure, the green line indicates 3 organ failures, the blue line indicates a CRP concentration of 300 mg/L and the black line indicates the scenario where both CRP and the level of organ failure are 300 mg/L and 3 respectively.
Abbrevations: *ORGF*, organ failure

Model Evaluation

The final model was evaluated in a bootstrap analysis. Median parameter values as well as the 5th and the 95th percentiles were in agreement with the model estimations and standard errors (Table III). Normal distribution of errors was shown in the normalized prediction distribution errors (NPDE), with no significant trends in NPDE versus time and NPDE versus predictions (Suppl. Fig. E2).

Dose simulations

Figure 4 shows simulated midazolam concentrations over time in the final PK model for patients with a body weight of 3.5, 10 and 60 kg. The simulations accounted for different clinical scenarios of increased CRP concentrations, increased organ failures or both increased CRP concentrations and organ failures. At a CRP level of 300 mg/L the plasma midazolam concentration is 2.7 fold higher than at a CRP level of 10 mg/L (Figure 4a-c). With three organ failures the plasma concentration is 1.5 fold higher than with one organ failure (Figure 4d-f). Plasma concentrations are

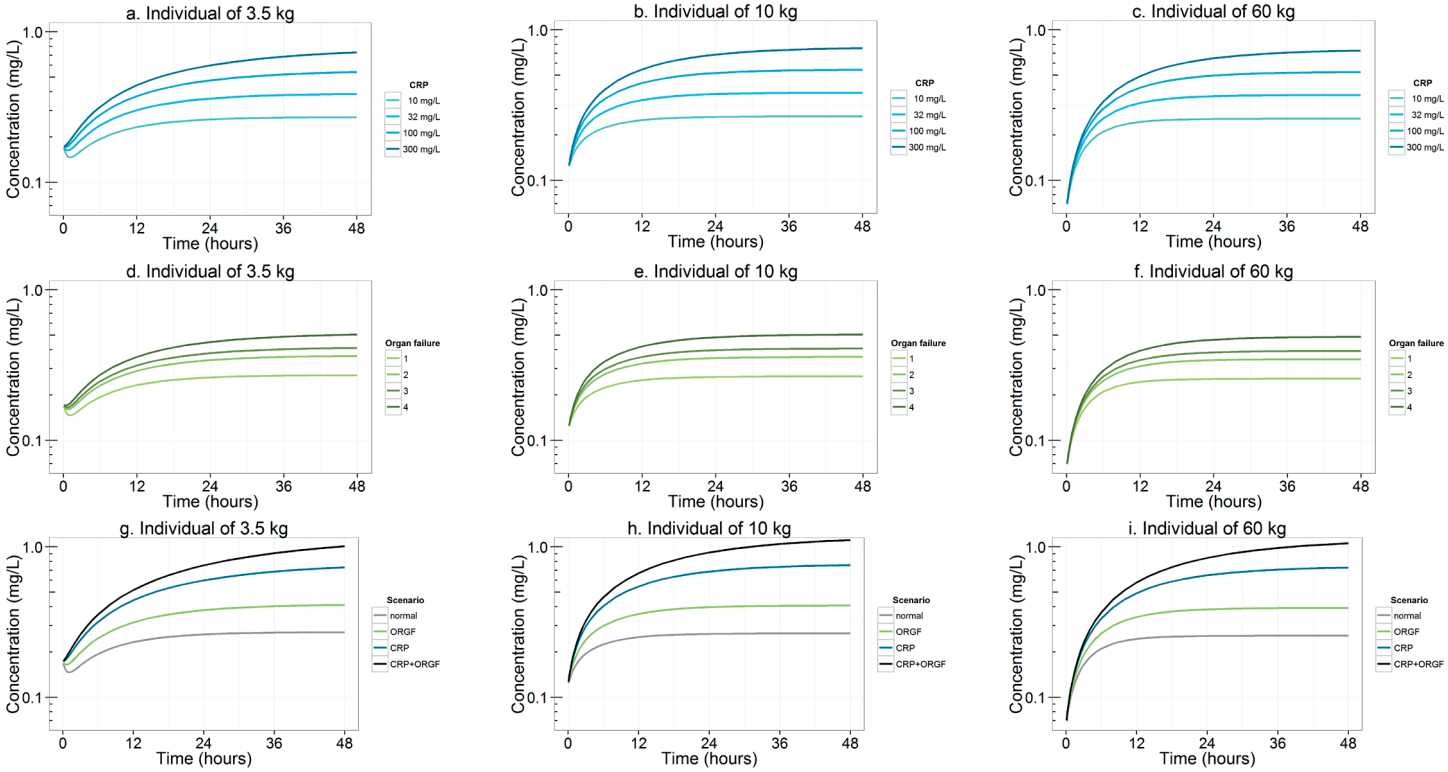

Figure 4. Simulations of midazolam concentration over time for three typical individuals in the study of 3.5, 10 and 60 kg, receiving a continuous infusion of 100 µg/kg/h for 48 hours and a loading dose of 100 µg/kg. (a-c) Concentration-time profiles for different CRP concentrations ranging from 10-300 mg/L. (d-f) Concentration-time profiles for different levels of organ failure. (g-i) Concentration-time profiles for the combined effect of different CRP concentrations and levels of organ failure (ORGF). The grey line represents the scenario when the patient has a CRP concentration of 10 mg/L and 1 organ failure, the green line indicates 3 organ failures, the blue line indicates CRP concentration of 300 mg/L and the black line indicates the scenario where both CRP and the level of organ failure are 300 mg/L and 3 respectively.

even higher in patients with both increased CRP concentration and higher number of organ failures (Figure 4g-l).

DISCUSSION

This prospective population PK study shows that both inflammation, as reflected by CRP, and disease severity, as reflected by the number of organ failures, significantly affect midazolam clearance in critically ill children. These data suggest that critically ill patients may be at an increased risk of increased drug levels and associated toxicity when receiving CYP3A substrate drugs.

Our study importantly adds to existing data. In septic critically ill children, antipyrine clearance, as global marker of CYP450 metabolism was related to inflammation and severity of organ failure (5). By using midazolam as validated probe of CYP3A activity, our data may serve to predict more specifically the impact of inflammation and organ failure on CYP3A activity, and thereby the clearance of specific CYP3A substrates. A previous study found lower midazolam clearance on average in critically children than in children receiving midazolam for elective procedures (17). The reason for this lower clearance remained unclear, and they speculated that inflammation may contribute to decreased CYP activity.

Also, in a pilot study we showed that organ failure as reflected by PELOD score, but not CRP, was related to midazolam clearance (9). Most likely, the lack of correlation with CRP was due to the small sample size in this pilot study (n=17). Together, these studies suggest an important effect of inflammation and/or critical illness on CYP3A-mediated drug metabolism in children, but did not make clear to what extent inflammation and organ failure affect drug metabolism and consequent clearance. Furthermore, these studies were restricted by number and range of patients and data. The present study includes a much larger cohort of critically ill children, covering an extensive variation in age, bodyweight, degree of inflammation and disease severity. Therefore, we were able to demonstrate the effect of inflammation and organ failure within a pediatric ICU population.

To support our hypothesis that inflammation-mediated mechanisms are related to the observed lower midazolam clearance, we determined cytokines and CRP. IL-6 is a principal inhibitor of CYP3A mRNA expression (18). In adult patients after elective surgery and bone marrow transplant, and in patients with rheumatoid arthritis and cancer, elevated IL-6 levels correlated with reduced CYP3A4 activity (19-22).

Furthermore, inhibition of IL-6 by the IL-6 inhibitor tocilizumab seemed to reverse this IL-6 mediated CYP3A downregulation in adult rheumatoid arthritis patients (23).

Indeed, in line with these studies and as we hypothesized, higher IL-6 levels were related to lower midazolam clearance. Moreover, C-reactive protein levels were also negatively correlated with midazolam clearance. CRP is an acute phase protein whose production by the liver is triggered by pro-inflammatory cytokines such as IL-6(24). This is apparent by the strong correlation between the IL-6 and CRP serum levels. As CRP explained more of the variability within patients, is clinically easily available and measured frequently, CRP was chosen as final parameter in our pharmacokinetic model.

Next to inflammation, the number of organ failures was significantly related to midazolam clearance and adding this covariate further improved the model. As midazolam has a low to intermediate hepatic extraction ratio, changes in hepatic clearance are predominantly dependent on CYP enzymes, but some impact of liver flow cannot be excluded (8, 25). Variation in liver flow in critically ill patients may result from changes in cardiac output consequent to cardiac failure and/or mechanical ventilation. Also, kidney failure has been associated with decreased hepatic drug metabolism (4). In contrast, in our study, creatinine levels, as markers of kidney function, were not significantly associated with reduced midazolam clearance, while in an adult study midazolam clearance was significantly lower in critically ill patients with acute kidney failure (26).

Hence, in addition to inflammation-mediated CYP3A downregulation, organ failure in itself may add to a reduction in midazolam clearance. This is supported by the 20% higher concentrations in the simulations when organ failure was added to the effect of CRP.

Apart from age and disease, genetic variation in CYP3A4/5 activity may contribute to variation in midazolam clearance. We could, however, not identify a significant effect of genetic polymorphisms of CYP3A4 and CYP3A5 on midazolam clearance. There was a trend but not significant lower clearance in patients with CYP3A4*22, possibly due to the low prevalence of this SNP in our cohort. Patients who expressed the CYP3A5*1 allele, i.e. who express functional CYP3A5, did not have a higher midazolam clearance. We also could not confirm that functional CYP3A5 compensates for CYP3A4 suppression, as previously suggested (26).

Some possible limitations of our study should be acknowledged. First, all patients had at least one organ failure (the lung) as mechanical ventilation was an inclusion criterion of the original study. Only in a few patients we could collect data in

the absence of organ failure (i.e. after extubation).Second, we did not determine midazolam metabolite pharmacokinetics, the knowledge of which could have further supported our hypothesis that CYP3A metabolism is reduced in sicker patients. Lastly, our data show an association between inflammation and midazolam clearance but a definite causal relationship could not be established due to the nature of the study. A controlled study was considered not feasible in this ICU setting.

Despite these limitations, our results strongly indicate that critically ill patients are at an increased risk of drug toxicity or therapy failure due to important inflammation and organ failure mediated variation in clearance of CYP3A substrates. As CYP2D6, CYP1A2, CYP2C9 and CYP2C19 also appear downregulated in response to inflammation, our results may have an even wider impact and warrant further study for these enzymes and their substrates (27-30). In daily practice, our results may support more extensive therapeutic drug monitoring in patients with unexplained symptoms potentially related to drug toxicity. Finally, similar to drug metabolizing enzymes, drug receptors may also be subject to changes related to critical illness and in turn alter sensitivity to the drug's effect (21). Hence, further exploration of the pharmacokinetic-pharmacodynamic relationship in critical illness is recommended.

ACKNOWLEDGEMENTS

The authors declare that they have no conflict of interest. We thank Ko Hagoort (Erasmus MC–Sophia Children's Hospital) for editorial assistance.

REFERENCES

1. Zuppa AF, Barrett JS. Pharmacokinetics and pharmacodynamics in the critically ill child. *Pediatric clinics of North America* 2008; 55: 735-755, xii.
2. Aitken AE, Richardson TA, Morgan ET. Regulation of drug-metabolizing enzymes and transporters in inflammation. *Annual review of pharmacology and toxicology* 2006; 46: 123-149.
3. Vet NJ, de Hoog M, Tibboel D, de Wildt SN. The effect of inflammation on drug metabolism: a focus on pediatrics. *Drug Discov Today* 2011; 16: 435-442.
4. Lalande L, Charpiat B, Leboucher G, Tod M. Consequences of renal failure on non-renal clearance of drugs. *Clin Pharmacokinet* 2014; 53: 521-532.
5. Carcillo JA, Doughty L, Kofos D, Frye RF, Kaplan SS, Sasser H, Burckart GJ. Cytochrome P450 mediated-drug metabolism is reduced in children with sepsis-induced multiple organ failure. *Intensive Care Med* 2003; 29: 980-984.

6. Aitken AE, Morgan ET. Gene-specific effects of inflammatory cytokines on cytochrome P450 2C, 2B6 and 3A4 mRNA levels in human hepatocytes. *Drug Metab Dispos* 2007; 35: 1687-1693.
7. Gorski JC, Hall SD, Jones DR, VandenBranden M, Wrighton SA. Regioselective biotransformation of midazolam by members of the human cytochrome P450 3A (CYP3A) subfamily. *Biochem Pharmacol* 1994; 47: 1643-1653.
8. Thummel KE, Shen DD, Podoll TD, Kunze KL, Trager WF, Hartwell PS, Raisys VA, Marsh CL, McVicar JP, Barr DM, et al. Use of midazolam as a human cytochrome P450 3A probe: I. In vitro-in vivo correlations in liver transplant patients. *J Pharmacol Exp Ther* 1994; 271: 549-556.
9. Vet NJ, de Hoog M, Tibboel D, de Wildt SN. The effect of critical illness and inflammation on midazolam therapy in children. *Pediatr Crit Care Med* 2012; 13: e48-50.
10. Vet NJ BJ, de Hoog M, Mooij MG, Verlaat CW, Tibboel D, Knibbe CA, de Wildt SN. Organ failure and C-reactive protein both affect midazolam clearance in critically ill children: a population PK model. Presented at the Biannual meeting of the ESDPPP, Belgrade, June 2015. http://www.esdp2015.org/images/Abstract_book.pdf
11. Vet NJ, de Wildt SN, Verlaat CW, Knibbe CA, Mooij MG, Hop WC, van Rosmalen J, Tibboel D, de Hoog M, Skic. Daily interruption of sedation in critically ill children: study protocol for a randomized controlled trial. *Trials* 2014; 15: 55.
12. Pollack MM, Ruttimann UE, Getson PR. Pediatric risk of mortality (PRISM) score. *Crit Care Med* 1988; 16: 1110-1116.
13. Shann F, Pearson G, Slater A, Wilkinson K. Paediatric index of mortality (PIM): a mortality prediction model for children in intensive care. *Intensive Care Med* 1997; 23: 201-207.
14. Leteurtre S, Martinot A, Duhamel A, Proulx F, Grandbastien B, Cotting J, Gottesman R, Joffe A, Pfenninger J, Hubert P, Lacroix J, Leclerc F. Validation of the paediatric logistic organ dysfunction (PELOD) score: prospective, observational, multicentre study. *Lancet* 2003; 362: 192-197.
15. Krekels EH, Neely M, Panoilia E, Tibboel D, Capparelli E, Danhof M, Mirochnick M, Knibbe CA. From pediatric covariate model to semiphysiological function for maturation: part I-extrapolation of a covariate model from morphine to Zidovudine. *CPT Pharmacometrics Syst Pharmacol* 2012; 1: e9.
16. Krekels EH, Johnson TN, den Hoedt SM, Rostami-Hodjegan A, Danhof M, Tibboel D, Knibbe CA. From Pediatric Covariate Model to Semiphysiological Function for Maturation: Part II-Sensitivity to Physiological and Physicochemical Properties. *CPT Pharmacometrics Syst Pharmacol* 2012; 1: e10.
17. Ince I, Knibbe CA, Danhof M, de Wildt SN. Developmental changes in the expression and function of cytochrome P450 3A isoforms: evidence from in vitro and in vivo investigations. *Clin Pharmacokinet* 2013; 52: 333-345.
18. Morgan ET, Goralski KB, Piquette-Miller M, Renton KW, Robertson GR, Chaluvadi MR, Charles KA, Clarke SJ, Kacevska M, Liddle C, Richardson TA, Sharma R, Sinal CJ. Regulation of drug-metabolizing enzymes and transporters in infection, inflammation, and cancer. *Drug Metab Dispos* 2008; 36: 205-216.
19. Haas CE, Kaufman DC, Jones CE, Burstein AH, Reiss W. Cytochrome P450 3A4 activity after surgical stress. *Crit Care Med* 2003; 31: 1338-1346.

20. Chen YL, Le Vraux V, Leneveu A, Dreyfus F, Stheneur A, Florentin I, De Sousa M, Giroud JP, Flouvat B, Chauvelot-Moachon L. Acute-phase response, interleukin-6, and alteration of cyclosporine pharmacokinetics. *Clin Pharmacol Ther* 1994; 55: 649-660.
21. Mayo PR, Skeith K, Russell AS, Jamali F. Decreased dromotropic response to verapamil despite pronounced increased drug concentration in rheumatoid arthritis. *Br J Clin Pharmacol* 2000; 50: 605-613.
22. Rivory LP, Slaviero KA, Clarke SJ. Hepatic cytochrome P450 3A drug metabolism is reduced in cancer patients who have an acute-phase response. *Br J Cancer* 2002; 87: 277-280.
23. Schmitt C, Kuhn B, Zhang X, Kivitz AJ, Grange S. Disease-drug-drug interaction involving tocilizumab and simvastatin in patients with rheumatoid arthritis. *Clin Pharmacol Ther* 2011; 89: 735-740.
24. Fulop AK. Genetics and genomics of hepatic acute phase reactants: a mini-review. *Inflamm Allergy Drug Targets* 2007; 6: 109-115.
25. Thummel KE, Shen DD, Podoll TD, Kunze KL, Trager WF, Bacchi CE, Marsh CL, McVicar JP, Barr DM, Perkins JD, et al. Use of midazolam as a human cytochrome P450 3A probe: II. Characterization of inter- and intraindividual hepatic CYP3A variability after liver transplantation. *J Pharmacol Exp Ther* 1994; 271: 557-566.
26. Kirwan CJ, MacPhee IA, Lee T, Holt DW, Philips BJ. Acute kidney injury reduces the hepatic metabolism of midazolam in critically ill patients. *Intensive Care Med* 2012; 38: 76-84.
27. Jones AE, Brown KC, Werner RE, Gotzkowsky K, Gaedigk A, Blake M, Hein DW, van der Horst C, Kashuba AD. Variability in drug metabolizing enzyme activity in HIV-infected patients. *European journal of clinical pharmacology* 2010; 66: 475-485.
28. Frye RF, Schneider VM, Frye CS, Feldman AM. Plasma levels of TNF-alpha and IL-6 are inversely related to cytochrome P450-dependent drug metabolism in patients with congestive heart failure. *J Card Fail* 2002; 8: 315-319.
29. Williams ML, Bhargava P, Cherrouk I, Marshall JL, Flockhart DA, Wainer IW. A discordance of the cytochrome P450 2C19 genotype and phenotype in patients with advanced cancer. *Br J Clin Pharmacol* 2000; 49: 485-488.
30. Helsby NA, Lo WY, Sharples K, Riley G, Murray M, Spells K, Dzhelai M, Simpson A, Findlay M. CYP2C19 pharmacogenetics in advanced cancer: compromised function independent of genotype. *Br J Cancer* 2008; 99: 1251-1255.
31. Beal SL. Ways to fit a PK model with some data below the quantification limit. *J Pharmacokinet Pharmacodyn* 2001; 28: 481-504.
32. Wang C, Peeters MY, Allegaert K, Blusse van Oud-Alblas HJ, Krekels EH, Tibboel D, Danhof M, Knibbe CA. A bodyweight-dependent allometric exponent for scaling clearance across the human life-span. *Pharm Res* 2012; 29: 1570-1581.
33. Comets E, Brendel K, Mentre F. Computing normalised prediction distribution errors to evaluate nonlinear mixed-effect models: the npde add-on package for R. *Comput Methods Programs Biomed* 2008; 90: 154-166.

SUPPLEMENTAL MATERIAL (CHAPTER 3)

Supplemental methods

Analytical methods

Midazolam plasma concentrations were measured using liquid chromatography-tandem mass spectrometry (LC-MS/MS), validated according to current ICH and FDA guidelines. The lower limit of quantification was 5.1 ng/ml. Serum cytokine levels were determined using a customized Luminex Performance Assay (R&D Systems) containing the following analytes: MCP-1, MIP1a, MIP1b, RANTES, IL-8, FGF-b, G-CSF, GM-CSF, IFN-γ, IL-1a, IL-1b, IL-2, IL-4, IL-6, IL-10, TNF-α. Samples were prepared according to the manufacturer's instructions, read on a BioPlex200 System, and analyzed in BioPlex Manager 6.0 software. CRP was measured using an immunoturbidimetric assay (Modular analytics <P> Roche diagnostics, Mannheim, Germany) and values <5 mg/L were considered normal. Genomic DNA was isolated from 200 Jl EDTA blood or saliva on the MagNA Pure Compact System with the use of MagNA Pure Compact Nucleic Acid Isolation Kit I (Roche®). The genetic variants CYP3A4*1G (rs2242480), *22 (rs35599367) and CYP3A5*3 (rs776746) were determined on the 7500 Real-Time PCR System (Applied Biosystems®) with the use of Taqman® SNP Genotyping Assay C__26201900_30, C__59013445_10 and C__26201809_30 (Applied Biosystems®), respectively.

Analysis of Pharmacokinetic Data

Population pharmacokinetic (PK) data analysis was performed using first-order conditional estimation with interaction in NONMEM version 7.3 (ICON, Globomax LLC, Ellicott, MD, USA) with Pirana 2.9.0 and R version 3.1.1 for visualization of data. Of all measurements, 1.3% were below the limit of quantification (BLQ). BLQ observations were handled according to the M6 method(35), as other methods did not result in an improvement of the model.

Model development

Model development was in four steps: (1) selection of a structural model, (2) selection of an error model, (3) covariate analysis and (4) internal validation of the model. For the structural and error models, a decrease in objective function value (OFV) of 3.84 points was considered statistically significant ($p<0.05$). Visual improvement of the goodness-of-fit plots (observed vs. individual and population predicted concentration, conditional weighted residuals (CWRES) vs. time and CWRES vs. population predicted concentration) was evaluated. In addition, the confidence interval for the estimated parameters, the correlation matrix, η-shrinkage and the

condition number (to find ill-conditioning or over-parameterization of the model) served to evaluate the models.

The individual pharmacokinetic parameters (post-hoc values) of the *i*th subject are modeled by use of Eq. 1:

(1) $P_i = P_{pop} \cdot e^{\eta_i}$

where P^i is the individual value of the PK parameters of the *i*th individual, P_{pop} the population prediction and η_i the inter-individual variability, which is assumed to be a Gaussian random variable with a mean zero and variance of ω^2 with a log-normal distribution. Inter-occasion variability on the different parameters was tested for the subsequent days to assess changes in pharmacokinetic parameters between days. This resulted in the identification of interoccasion variability (IOV) on clearance describing the changes in clearance within individuals during the study according to Eq. 2:

(2) $CL_{ij} = CL_{pop} \cdot e^{\eta_i + m_{ij}}$

where CL_{ij} is the individual parameter estimate at the *j*th occasion, CL_{pop} the population prediction of clearance, η_i the inter-individual variability and m_{ij} is a random variable for the *i*th individual at the *j*th occasion (IOV). Both ηi and mij were assumed to be independently normally distributed with a mean of zero and variances ω2 and π2, respectively. The IOV represents the variability between different occasions, where every 24 hours after the first dose was regarded as a new occasion. The residual unexplained variability was described with a combined error model (proportional and additive error model) for all data. The observations of the *j*th observation of the *i*th individual are described according to Eq. 3:

(3) $Y_{ij} = C_{pred,ij} \cdot (1 + \varepsilon_1) + \varepsilon_2$

where Y_{ij} is the observed concentration, $C_{pred,ij}$ the predicted concentration for the *j*th observation in the *i*th individual and ε_1 and ε_2 the proportional and additive error samples respectively from a distribution with a mean of zero and variance of σ^2.

Covariate Analysis

Tested covariates included patient characteristics (age, weight, sex, diagnosis group, coadministration of CYP3A inhibitors, study center, CYP3A polymorphisms), inflammation markers (CRP, cytokines) and disease severity (PRISM II, PIM2, PELOD, number of organ failures, creatinine, ALAT and albumin). Individual post-hoc parameters, inter-individual variability and conditionally weighted residuals (CWRES) were plotted against the covariates to evaluate possible relationships. Continuous covariates were tested in a linear or power function (Eqs. 4 and 5):

(4) $P_i = P_{pop} \cdot \left(1 + \left(\frac{Cov_i}{Cov_{median}}\right) \cdot l\right)$

$$P_i = P_{pop} \cdot \left(\frac{Cov_i}{Cov_{median}}\right)^k \quad (5)$$

where P_i and Cov_i are the values for the parameter and covariate, respectively, for the *i*th individual, P_{pop} is the population mean for parameter P and Cov_{median} is the standardized value of the covariate. In the linear function, the slope is depicted by *l*. For Eq. 5, *k* represents the scaling factor in the power function. For clearance, also a body weight dependent exponent *k* was tested(36). Since the concentration of IL-6 covered a large range, it was log-transformed and as such considered as covariate in the model. Categorical covariates such as co-administration of CYP3A inhibitors, sex and number of organs failing were tested as a fraction for each category or independently estimated for the different categories. When a CYP3A inhibitor (i.e. clarithromycin, voriconazole, fluconazole, erythromycin, haloperidole, metronidazole) was administered at the same day as midazolam, a factor affecting clearance was estimated for that day. Potential covariates were evaluated using forward inclusion and backward elimination with a level of significance of <0.005 (OFV -7.9 points) and <0.001 (OFV -10.8 points), respectively. In addition, inclusion of a covariate in the model had to result in a decline in unexplained inter-individual variability or unexplained inter-occasion variability before it was included in the final model(18, 19). Additional covariates had to reduce the objective function and unexplained variability further to be retained in the model.

Model Evaluation

The model was internally validated using bootstrap analysis in Perl-speaks-NONMEM (PsN version 4.2.0). Five hundred datasets were resampled from the original datasets and refitted to the model. Normalized prediction distribution errors (NPDE) were calculated with the NPDE package in R(37). For this method, the dataset used for model development was simulated a thousand times with inclusion of inter-individual and inter-occasion variability and residual error.

SUPPLEMENTAL FIGURES

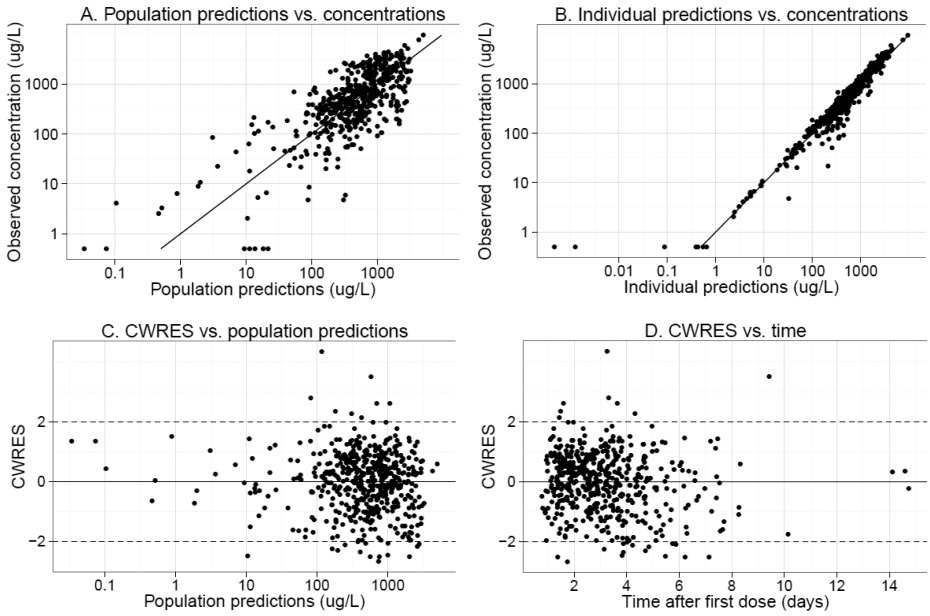

Figure E1. Goodness-of-fit plots for the final model with inflammation and organ failure included as covariates. A. Log observed plasma concentrations vs. log population predicted concentrations. B. Log observed plasma concentrations vs. log individual predicted concentrations on a log scale. C. Conditional weighted residuals (CWRES) versus log population predictions. D. CWRES versus time after first dose.

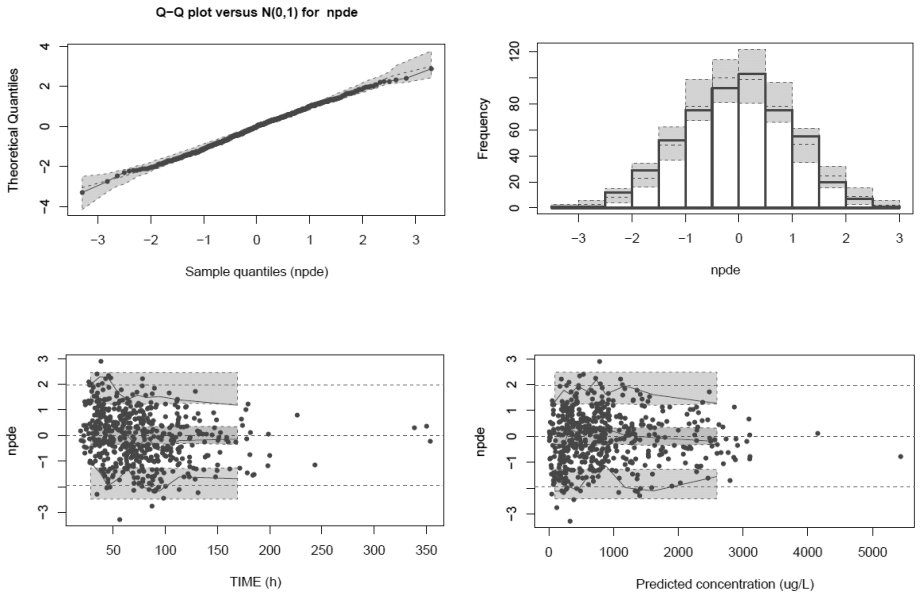

Figure E2. Normalized prediction distribution error (NPDE) results of the final model with inflammation and disease severity included as covariate plots. A. Q-Q plot. B. Histogram of the NPDE distribution. C. NPDE versus time after first dose in hours. D. NPDE versus predicted concentrations in µg/L.

REFERENCES

1. Beal SL. Ways to fit a PK model with some data below the quantification limit. *J Pharmacokinet Pharmacodyn* 2001; 28: 481-504.
2. Wang C, Peeters MY, Allegaert K, Blusse van Oud-Alblas HJ, Krekels EH, Tibboel D, Danhof M, Knibbe CA. A bodyweight-dependent allometric exponent for scaling clearance across the human life-span. *Pharm Res* 2012; 29: 1570-1581.
3. Krekels EH, Neely M, Panoilia E, Tibboel D, Capparelli E, Danhof M, Mirochnick M, Knibbe CA. From pediatric covariate model to semiphysiological function for maturation: part I-extrapolation of a covariate model from morphine to Zidovudine. *CPT Pharmacometrics Syst Pharmacol* 2012; 1: e9.
4. Krekels EH, Johnson TN, den Hoedt SM, Rostami-Hodjegan A, Danhof M, Tibboel D, Knibbe CA. From Pediatric Covariate Model to Semiphysiological Function for Maturation: Part II-Sensitivity to Physiological and Physicochemical Properties. *CPT Pharmacometrics Syst Pharmacol* 2012; 1: e10.
5. Comets E, Brendel K, Mentre F. Computing normalised prediction distribution errors to evaluate nonlinear mixed-effect models: the npde add-on package for R. *Comput Methods Programs Biomed* 2008; 90: 154-166.